

## The liquid-crystalline phase behaviour of hard spherocylinders with terminal point dipoles

This article has been downloaded from IOPscience. Please scroll down to see the full text article.

1996 J. Phys.: Condens. Matter 8 9649

(<http://iopscience.iop.org/0953-8984/8/47/078>)

View [the table of contents for this issue](#), or go to the [journal homepage](#) for more

Download details:

IP Address: 171.66.16.207

The article was downloaded on 14/05/2010 at 05:40

Please note that [terms and conditions apply](#).

# The liquid-crystalline phase behaviour of hard spherocylinders with terminal point dipoles

Simon C McGrother, Alejandro Gil-Villegas and George Jackson

Department of Chemistry, University of Sheffield, Sheffield S3 7HF, UK

Received 15 July 1996, in final form 26 August 1996

**Abstract.** We examine the effect of dipolar interactions on the liquid-crystalline phase behaviour of  $L/D = 5$  hard spherocylinders with a terminal point dipole. The hard spherocylinder consists of a cylinder of length  $L$  and diameter  $D$  with hemispherical caps on each end; the point dipole is located at the centre of the hemispherical cap ( $2.5D$  from the centre of the spherocylinder) and is oriented along the principal molecular axis. The phase transitions exhibited by this system are studied using the isothermal–isobaric Monte Carlo (MC-*NPT*) technique. As for systems with central dipoles, the terminal dipole is seen to slightly destabilize the nematic (orientationally ordered) phase relative to the isotropic phase when compared with the non-polar hard spherocylinders. More interestingly, the smectic (layered) phase is destabilized in the terminal dipole case, and is only seen at the very highest densities. This is in stark contrast to what is seen for systems with central point dipoles in which the smectic phase is stabilized relative to the nematic phase due to the strong anti-parallel dipolar interactions. We do not find any evidence for ferroelectric or anti-ferroelectric ordering in these systems.

## 1. Introduction

The relationship between polar interactions and liquid-crystalline phase behaviour has been of long-standing interest since the pioneering work of Born [1]. There have been numerous theoretical and simulation studies for systems with dipolar interactions (e.g., see [2–29]). The main findings of this body of work are that the dipole stabilizes the nematic (N) phase relative to the isotropic (I) liquid, and that ferroelectric phases can be observed. Recently, we have undertaken a thorough simulation study of the phase transitions of hard spherocylinders of aspect ratio  $L/D = 5$  with central point dipoles in a longitudinal [30] and transverse [31] orientation relative to the main molecular axis. In these systems the smectic-A (SmA) phase is seen to be stabilized when compared with the results for the non-polar hard spherocylinders [32]. Contrary to theoretical expectations, the nematic phase was found to be destabilized relative to both the isotropic liquid and the smectic phases. Furthermore, we did not observe the formation of ferroelectric liquid-crystalline phases.

In this contribution, we examine  $L/D = 5$  hard spherocylinders with a terminal dipole located at the centre of the hemispherical cap, a distance  $2.5D$  from the centre of the spherocylinder; the orientation of the dipole is along the principal axis of the cylinder. This system has already been studied for a limited number of states [18, 19]. Much of the motivation behind our work is the study of Vanakaras and Photinos [10] who predict I–N–I re-entrance with a variational theory for a variety of positions of the dipole within the spherocylinder. We will briefly discuss the specific details of our simulation technique before the results of our study are presented.

## 2. Simulation details

As in our previous work on hard spherocylinders [32], we use the isothermal–isobaric Monte Carlo (MC-*NPT*) method [33, 34]. This constant-pressure simulation technique is well established and is very convenient for studies of phase transitions as the density of the system is not fixed. The reaction-field method [34, 35, 36] is used to deal with the long-range dipolar interactions; the dielectric continuum at the boundary is calculated from within the simulation cell in a self-consistent manner [37]. We have shown [37] that for the liquid-crystalline phases of dipolar hard spherocylinders, at least, the thermodynamics and structure obtained with this procedure are indistinguishable from those obtained with the more commonly used, but more computationally intensive, Ewald summation method [34].

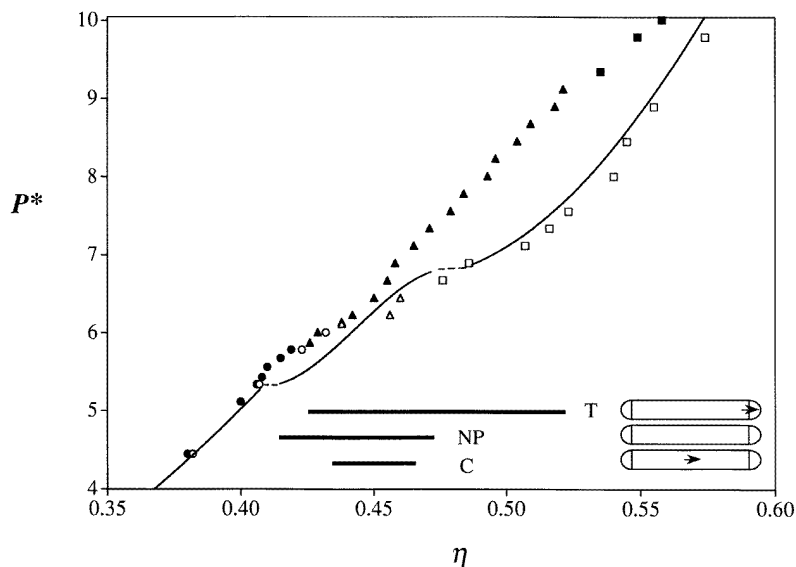


**Figure 1.** The equation of state for dipolar hard spherocylinders with  $L/D = 5$  for the isotherm  $T^* = 1$ . The data points represent the MC-*NPT* simulation data for  $N = 1020$  particles: the circles correspond to the isotropic branch, the triangles to the nematic branch, and the squares to the smectic branch. The data points for the system with the terminal (T) longitudinal dipole are shown black, and those for the system with the central (C) longitudinal dipole white [30]. The continuous curves represent the results for the non-polar (NP)  $L/D = 5$  hard spherocylinders [32]: isotropic, nematic, and then smectic branches are seen with increasing density. The ranges of stability of the nematic phase for these systems are also shown as the thick solid lines.

A single isotherm of  $T^* = kTD^3/\mu^2 = 1$  is examined for the system with terminal dipoles, where  $T$  is the temperature,  $k$  is the Boltzmann constant, and  $\mu$  is the dipole moment. This temperature has been selected since both nematic and smectic-A phases are found for the systems with central longitudinal dipoles [30]. At the start of the simulation, a system of  $N = 1020$  molecules are arranged on a near-cubic hexagonally close-packed (hcp) lattice which is then expanded to a low-density isotropic state [32]. The system is equilibrated at this point so that all of the orientational order is lost, and the reduced pressure  $P^* = Pv_{\text{hsc}}/(kT)$ , where  $P$  is the pressure and  $v_{\text{hsc}} = \pi D^3/6 + \pi LD^2/4$  is the volume of the hard spherocylinder, is gradually increased (from a low-density value) in a series of simulations to give the full isotherm and allow us to locate the various phase transitions.

**Table 1.** Isothermal–isobaric Monte Carlo (MC-*NPT*) simulation results for  $N = 1020$  hard spherocylinders of aspect ratio  $L/D = 5$  with a terminal longitudinal dipole at a temperature of  $T^* = 1$ . The pressure  $P^*$  is set during the simulation and the packing fraction  $\eta$ , internal energy  $U^*$ , and order parameters  $P_1$  (ferroelectric) and  $P_2$  (nematic) are obtained as configurational averages; the uncertainties denote one standard deviation of the data.

$P^*$	$\eta$	$U^*$	$P_1$	$P_2$	Phase
4.451	0.380 ± 0.001	−0.0755 ± 0.006	0.0008 ± 0.025	0.033 ± 0.004	I
5.118	0.400 ± 0.001	−0.0724 ± 0.005	−0.0017 ± 0.014	0.119 ± 0.004	I
5.341	0.406 ± 0.001	−0.0713 ± 0.004	0.0051 ± 0.072	0.194 ± 0.005	I
5.430	0.408 ± 0.001	−0.0745 ± 0.005	−0.0002 ± 0.005	0.195 ± 0.003	I
5.563	0.410 ± 0.001	−0.0732 ± 0.003	0.0016 ± 0.011	0.194 ± 0.005	I
5.675	0.415 ± 0.001	−0.0734 ± 0.006	0.0024 ± 0.008	0.237 ± 0.004	I
5.786	0.419 ± 0.001	−0.0656 ± 0.007	0.0006 ± 0.012	0.220 ± 0.015	I
5.875	0.426 ± 0.001	−0.0611 ± 0.006	−0.0004 ± 0.006	0.438 ± 0.005	N
6.008	0.429 ± 0.002	−0.0608 ± 0.006	0.0003 ± 0.005	0.485 ± 0.004	N
6.142	0.438 ± 0.002	−0.0539 ± 0.007	−0.0004 ± 0.005	0.685 ± 0.004	N
6.231	0.442 ± 0.002	−0.0518 ± 0.008	−0.0006 ± 0.005	0.731 ± 0.003	N
6.453	0.450 ± 0.001	−0.0433 ± 0.009	−0.0002 ± 0.006	0.791 ± 0.003	N
6.676	0.455 ± 0.002	−0.0446 ± 0.009	−0.0008 ± 0.006	0.810 ± 0.004	N
6.898	0.458 ± 0.002	−0.0409 ± 0.010	0.0010 ± 0.006	0.791 ± 0.003	N
7.121	0.465 ± 0.001	−0.0346 ± 0.011	0.0005 ± 0.006	0.817 ± 0.003	N
7.343	0.471 ± 0.001	−0.0319 ± 0.011	−0.0012 ± 0.005	0.839 ± 0.003	N
7.566	0.479 ± 0.003	−0.0209 ± 0.012	0.0017 ± 0.005	0.876 ± 0.002	N
7.788	0.484 ± 0.001	−0.0204 ± 0.012	0.0010 ± 0.005	0.872 ± 0.003	N
8.011	0.493 ± 0.001	−0.0086 ± 0.013	0.0027 ± 0.005	0.880 ± 0.003	N
8.234	0.496 ± 0.002	−0.0063 ± 0.014	−0.0006 ± 0.006	0.895 ± 0.003	N
8.456	0.504 ± 0.001	0.0037 ± 0.014	0.0004 ± 0.006	0.913 ± 0.002	N
8.679	0.509 ± 0.002	0.0075 ± 0.014	0.0007 ± 0.005	0.924 ± 0.002	N
8.901	0.518 ± 0.002	0.0183 ± 0.015	−0.0002 ± 0.007	0.942 ± 0.003	N
9.124	0.521 ± 0.001	0.0199 ± 0.014	0.0085 ± 0.010	0.939 ± 0.003	N
9.346	0.535 ± 0.002	0.0471 ± 0.019	0.0037 ± 0.024	0.961 ± 0.003	Sm
9.791	0.549 ± 0.001	0.0646 ± 0.017	0.0012 ± 0.009	0.967 ± 0.002	Sm
10.014	0.558 ± 0.002	0.0657 ± 0.021	−0.0006 ± 0.005	0.972 ± 0.002	Sm

At each state point, the system is equilibrated for  $\sim 4 \times 10^8$  configurations, and a further  $\sim 4 \times 10^8$  configurations are used to obtain the appropriate ensemble averages. Since the pressure  $P^*$  is set in an MC-*NPT* simulation, the equation of state is obtained from the average volume  $V$  or packing fraction  $\eta = v_{\text{hsc}}N/V$ . The thermodynamic and structural properties are monitored to characterize the various phases and to locate the positions of the phase transitions: the internal energy  $U^* = UD^3/\mu^2$ , the nematic  $P_2 = \langle P_2(\cos \theta) \rangle$  and ferroelectric  $P_1 = \langle P_1(\cos \theta) \rangle$  order parameters (where  $\theta$  is the angle between the molecular axis and the director), the pair distribution functions  $g_{lmn}(r)$ , projections of these functions for directions parallel  $g_{\parallel}(r_{\parallel})$  and perpendicular  $g_{\perp}(r_{\perp})$  to the director, and the orientational pair distribution functions  $g_n(r) = \langle P_n(\cos \theta(r)) \rangle / g_{000}(r)$  are calculated as described in our other papers [32, 30, 31].

### 3. Results and discussion

The Monte Carlo simulation data obtained for the  $L/D = 5$  hard spherocylinders with a terminal point dipole for the temperature  $T^* = 1.0$  are reported in table 1. These data are compared with the results for the non-polar case ( $T^* = \infty$ ) [32] in figure 1. The

simulation data obtained for the same isotherm of  $L/D = 5$  hard spherocylinders with a central longitudinal dipole [30] are also included in the figure.

The non-polar system exhibits a transition from an isotropic liquid phase ( $\eta_I \sim 0.407$ ,  $P_2 \sim 0.215$ ) to a nematic phase ( $\eta_N \sim 0.415$ ,  $P_2 \sim 0.471$ ) at a pressure of  $P_{I-N}^* \sim 5.30$ ; on further compression the system exhibits a layering transition from a nematic phase ( $\eta_N \sim 0.472$ ,  $P_2 \sim 0.857$ ) to a smectic-A phase ( $\eta_{SmA} \sim 0.487$ ,  $P_2 \sim 0.893$ ) at a pressure of  $P_{N-SmA}^* \sim 6.85$ . There is also a transition to a solid phase at higher densities, but this is not the focus of the current paper.

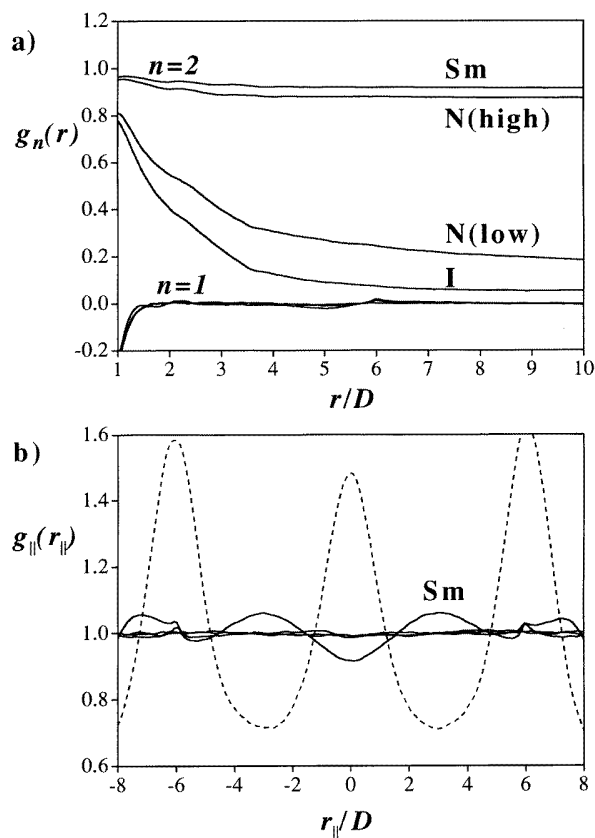


**Figure 2.** (a) The orientational pair radial distribution function for the  $L/D = 5$  hard spherocylinders with a terminal point dipole for a temperature of  $T^* = 1$ . The upper curves correspond to  $g_2(r)$  for the highest-density isotropic (I,  $P^* = 5.786$ ), the lowest-density nematic (N(low),  $P^* = 5.875$ ), the highest-density nematic (N(high),  $P^* = 9.124$ ), and the lowest-density smectic (Sm,  $P^* = 9.346$ ) phases. The lower curves correspond to  $g_1(r)$  for the same state points. (b) The projection  $g_{\parallel}(r_{\parallel})$  of the pair radial distribution function for a distance  $r_{\parallel}$  along the director. The continuous curves correspond to the same states as in (a). The results for the  $L/D = 5$  hard spherocylinders with a central transverse point dipole at the same temperature and  $P^* = 6.542$  are shown as the dashed curve.

At a temperature of  $T^* = 1.0$ , the hard spherocylinders with the terminal dipoles are seen to exhibit a transition from an isotropic liquid ( $\eta_I \sim 0.419$ ,  $P_2 \sim 0.220$ ,  $P_1 \sim 0.0006$ ) to a nematic phase ( $\eta_N \sim 0.426$ ,  $P_2 \sim 0.438$ ,  $P_1 \sim -0.0004$ ) at a pressure of  $P_{I-N}^* \sim 5.83$ . The nematic phase is not ferroelectric, i.e.,  $P_1 \sim 0$  over its entire range (see table 1).

The orientational pair distribution functions  $g_n(r)$  for various state points of this system are shown in figure 2(a):  $g_2(r)$  decays to zero with the intermolecular separation in the isotropic liquid, whilst it exhibits the limiting value of  $\lim_{r \rightarrow \infty} g_2(r) = P_2^2$  in the nematic phase; the decay of  $g_1(r)$  to zero indicates that the phases are not ferroelectric. The nematic phase is slightly destabilized with respect to the isotropic liquid when compared with the non-polar system; the polar system has a higher pressure and density and a lower nematic order parameter for the I–N transition. This rather surprising finding is also seen for the hard spherocylinders with central point dipoles [30], and could be due to dipole pairing (or clustering) reducing the overall aspect ratio of the molecular aggregates. The subtle effect is not reproduced in the theoretical predictions of Vanakaras and Photinos [10].

The most surprising feature of the phase behaviour of the hard spherocylinders with terminal dipoles, however, is the marked destabilization of the smectic phase relative to the nematic phase when compared with the non-polar system. We find a transition from a nematic phase ( $\eta_N \sim 0.521$ ,  $P_2 \sim 0.939$ ,  $P_1 \sim 0.0085$ ) to a poorly characterized smectic phase ( $\eta_{Sm} \sim 0.535$ ,  $P_2 \sim 0.961$ ,  $P_1 \sim 0.0037$ ) at a pressure of  $P_{N-Sm}^* \sim 9.24$ , which is well above the N–SmA transition pressure of  $P_{N-SmA}^* \sim 6.85$  found for the non-polar system [32]. One of the main features of the phase behaviour of hard spherocylinders with central dipoles is the marked stabilization of the smectic-A phase [30] (see figure 1). The ranges of stability of the nematic phase for the non-polar and dipolar (terminal and central) systems are indicated in figure 1 to emphasize this point. The layering can be characterized in terms of the pair distribution function for distances projected along the director  $g_{\parallel}(r_{\parallel})$ . This function is shown in figure 2(b) for states just below and above the N–Sm phase transition. Clear layering can be seen for a density of  $\eta = 0.535$ , but the layers are less well defined than for the systems with central dipoles; the corresponding sharp peaks for a typical smectic-A phase of the system with a transverse central dipole [31] is shown in figure 2(b) for the sake of comparison. We have found a slight tilt of the layers relative to the director for the high-density system with a terminal dipole, so the phase may be a smectic-C one. It is important to note, however, that this poorly characterized smectic phase could be metastable and preempted by a transition to a solid phase, although this possibility has not been investigated here. The destabilization of the smectic phase appears to be due to the strong anti-parallel dipole pairing at high densities which produces a staggered dimer geometry; these aggregates are difficult to accommodate in the smectic layers. The ‘dipole pairs’ have to be disrupted in order for the smectic phase to form. In this context, it is interesting to examine the pressure dependence of the internal energy  $U^*$  for this system (see table 1): the energy is less attractive (more repulsive) in the nematic than the isotropic case which agrees with the view that the nematic phase is destabilized. The opposite trend is found for the systems with central dipoles [30, 31]. The extra repulsions for the terminal case are due to the disruption of the dipole pairs; in fact the high-density system is more repulsive on average than the non-polar case as testified by the positive values of the internal energy. Like the nematic phase, the smectic phase does not appear to exhibit appreciable ferroelectric or anti-ferroelectric order, although some short-range anti-ferroelectric order can be seen (see figure 2(a)).

#### 4. Conclusions

Our main finding for hard spherocylinders with terminal dipoles is the dramatic stabilization of the nematic phase relative to the smectic phase in comparison with the non-polar system. This appears to be a consequence of the anti-parallel geometry of the dipoles in their minimum-energy conformation causing a staggering of the molecules which cannot then

easily be accommodated into smectic layers. This is in marked contrast to what is found for the systems with central dipoles in which the smectic phase is stabilized to such an extent that the nematic phase disappears altogether at low temperatures [30, 31]. It should be noted that we have not found evidence of ferroelectric or anti-ferroelectric phase behaviour. This type of behaviour is, however, very subtle and can depend on the types of boundary condition that are used, so that it cannot be ruled out.

So far we have made no reference to vapour–fluid phase equilibria. In a previous study [29] it was found that hard spherocylinders with central point dipoles exhibit a vapour–liquid phase transition only over a very narrow range of aspect ratios ( $0.18 < L/D < 0.28$ ). We do not thus expect a vapour–liquid transition for the molecules with the longer aspect ratio of  $L/D = 5$  although it is difficult to speculate on what will happen for these very much longer molecules especially in the case of the terminal dipoles.

The dipolar hard spherocylinders are, of course, a rather crude model of real mesogens such as the cyanobiphenyls (CB). In this case the cyano group is directly attached to the phenyl ring which results in a delocalized ‘dipole’ [38, 39]. When the cyano group is linked to a cyclohexyl ring, the dipole is more localized and the liquid-crystalline phases, the smectic phase in particular, are destabilized [38], an effect which is reproduced in our study. We have not included a representation of the flexible alkyl tails in our models due to the enhanced computational effort that is required in this case. In future work we plan to include this contribution and examine the competing effects of the pairing of the terminal dipoles and the flexible tails on the stability of the smectic phase and microphase separation.

## Acknowledgments

We would like to thank Jane C Hall for her help in developing the code. We are also very grateful to Demetri Photinos and his group for a hugely enjoyable and stimulating visit to Patras, and to the EC Human Capital and Mobility Network (CHRX-C193-0161) for funding. SCM and AGV acknowledge support from the Engineering and Physical Sciences Research Council (EPSRC) for the award of a studentship and a research fellowship. Funds for computer hardware have been provided by the European Commission (CII\*-CT94-0132), the Royal Society, and the ROPA Initiative of the EPSRC.

## References

- [1] Born M 1916 *Sitz. Phys. Math.* **25** 614; 1918 *Ann. Phys.* **55** 221
- [2] Maier W and Saupe A 1958 *Z. Naturf.* a **13** 564; 1959 *Z. Naturf.* a **14** 882; 1960 *Z. Naturf.* a **15** 287
- [3] Perera A and Patey G N 1988 *J. Chem. Phys.* **89** 5861  
Perera A, Patey G N and Weis J J 1988 *J. Chem. Phys.* **89** 6941
- [4] Palfy-Muhoray P, Lee M A and Petschek R G 1988 *Phys. Rev. Lett.* **60** 2303
- [5] Photinos D J, Poon C D, Samulski E T and Toriumi H 1992 *J. Phys. Chem.* **96** 8176
- [6] Netz R R and Berker A N 1992 *Phys. Rev. Lett.* **68** 333
- [7] Vega C and Lago S 1994 *J. Chem. Phys.* **56** 6727
- [8] Photinos D J and Samulski E T 1995 *Science* **270** 5237
- [9] Terzis A F and Photinos D J 1994 *Mol. Phys.* **83** 847
- [10] Vanakaras A G and Photinos D J 1995 *Mol. Phys.* **85** 1089
- [11] Rjuntsev E I, Osipov M A, Rotinyan T A and Yevlampieva N P 1995 *Liq. Cryst.* **18** 87
- [12] Sear R P 1996 *Phys. Rev. Lett.* **76** 2310
- [13] Zarragoicoechea G J, Levesque D and Weis J J 1991 *Mol. Phys.* **74** 629
- [14] Zarragoicoechea G J, Levesque D and Weis J J 1992 *Mol. Phys.* **75** 989
- [15] Weis J J, Levesque D and Zarragoicoechea G J 1992 *Phys. Rev. Lett.* **69** 913
- [16] Wei D Q and Patey G N 1992 *Phys. Rev. A* **46** 7783

- [17] Wei D Q and Patey G N 1992 *Phys. Rev. Lett.* **68** 2043
- [18] Levesque D, Weis J J and Zarragoicoechea G J 1993 *Phys. Rev. E* **47** 496
- [19] Weis J J, Levesque D and Zarragoicoechea G J 1993 *Mol. Phys.* **80** 1077
- [20] Levesque D and Weis J J 1993 *Phys. Rev. Lett.* **71** 2729
- [21] Weis J J and Levesque D 1993 *Phys. Rev. E* **48** 3728
- [22] Wei D Q, Patey G N and Perera A 1993 *Phys. Rev. E* **47** 506
- [23] Caillol J-M 1993 *J. Chem. Phys.* **98** 9835
- [24] van Leeuwen M E and Smit B 1993 *Phys. Rev. Lett.* **71** 3991
- [25] Levesque D and Weis J J 1994 *Phys. Rev. E* **49** 5131
- [26] Stevens M J and Grest G S 1994 *Phys. Rev. Lett.* **72** 3686
- [27] Stevens M J and Grest G S 1995 *Phys. Rev. E* **50** 5976
- [28] Satoh K, Mita S and Kondo S 1996 *Liq. Cryst.* **20** 757
- [29] McGrother S C and Jackson G 1996 *Phys. Rev. Lett.* **76** 4183
- [30] McGrother S C, Gil-Villegas A and Jackson G 1996 *Mol. Phys.* to be submitted
- [31] Gil-Villegas A, McGrother S C and Jackson G 1996 *Phys. Rev. E* to be submitted
- [32] McGrother S C, Williamson D C and Jackson G 1996 *J. Chem. Phys.* **104** 6755
- [33] Wood W W 1968 *J. Chem. Phys.* **48** 415
- [34] Allen M P and Tildesley D J 1987 *Computer Simulation of Liquids* (New York: Oxford University Press)
- [35] Onsager L 1936 *J. Am. Chem. Soc.* **58** 1486
- [36] Barker J A and Watts O R 1969 *Chem. Phys. Lett.* **3** 144
- [37] Gil-Villegas A, McGrother S C and Jackson G 1996 in preparation
- [38] Goodby J W 1991 *Ferroelectric Liquid Crystals* (Amsterdam: Gordon and Breach)
- [39] Vertogen G and de Jeu W H 1988 *Thermotropic Liquid Crystals, Fundamentals* (Berlin: Springer)